Research Journal of Applied Sciences, Engineering and Technology 14(3): 119-123, 2017
DOI:10.19026/rjaset.14.4154
ISSN: 2040-7459; e-ISSN: 2040-7467

Submitted: November 29, 2016 Accepted: January 30, 2017 Published: March 15, 2017

Research Article

Analysis of Residual Stresses in High Speed Milled Aluminum Alloys

[1]S. Vottero, [1]F.V. Díaz, [1]C.A. Mammana and [2]A.P.M. Guidobono
[1]Departamento de Ingeniería Electromecánica-Departamento de Ingeniería Industrial, Facultad Regional Rafaela, Universidad Tecnológica Nacional, Acuña 49, 2300 Rafaela, Argentina
[2]División Metrología Dimensional, Centro Regional Rosario (INTI), Ocampo y Esmeralda, 2000 Rosario, Argentina

Abstract: The purpose of this study is to evaluate, from high speed machining tests, the behavior of the residual stresses induced in samples of AA 6082-T6 and AA 7075-T6 aluminum alloys. This study includes an exhaustive analysis of residual stress anisotropy from diameters of Mohr's circles. The combination of process parameters was modified in order to evaluate the stress changes introduced in different zones of the surfaces generated. A method of micro-indents, which includes the adaptation of a universal measuring machine, was used to determine, with high accuracy, the normal components of residual stress in several directions. The obtained results reveal that although, in the alloy 7075-T6, the normal components are lower, in the alloy 6082-T6, these normal components tend to be grouped into smaller intervals and also, to show a more homogeneous directional behavior when the cutting conditions are more severe.

Keywords: Aluminum alloys, high speed machining, indent method, Mohr's circle, residual stresses

INTRODUCTION

In the last decades, High Speed Machining (HSM) has been the focus of numerous studies and advances in order to achieve highest levels of quality and productivity in manufacturing (Schulz, 1996; Cus *et al*., 2007; Pare *et al*., 2015). The increase of the HSM parameters, associated with the development and inclusion of new machine tools in industry, has allowed to obtain best machined components in more limited times. Furthermore, these advances have promoted the research for more resistant materials, able to withstand extreme conditions of machining.

However, residual stresses are introduced, inevitably, during the HSM of a mechanical component (Brinksmeier *et al*., 1982; Rao and Shin, 2001; Yao *et al*., 2012). This type of stresses can cause adverse effects on both the geometry and the life in service of different machined components. Due to this, the residual stresses must be studied exhaustively in the HSM regime. These stresses are caused by the plastic deformation generated by the interaction between the cutting tool and the material and also, by the heat conducted from the primary deformation zone to the surface generated (M'Saoubi *et al*., 2008; Abrão *et al*., 2011). It is important to note that these stresses are a function of the thermal and mechanical properties of the machined material, of the process parameters, of the geometry, design and cutting tool state and besides of the cooling conditions.

The purpose of this study is to evaluate and compare the behavior of the residual stresses induced in samples of AA 6082-T6 and AA 7075-T aluminum alloys subjected to HSM. In this study, HSM tests consisted of face milling operations with central cutting. These tests were carried out on a numerically controlled vertical milling machine. It is noteworthy that the central cutting allows to differentiate, in the surface generated, two adjacent zones: the conventional and climb cutting zones (Trent, 1991; Díaz *et al*., 2012). The depth of cut was varied in order to evaluate the differences in the behavior of the residual stresses, either between the cutting zones as well as between the different alloys. Furthermore, from a preliminary analysis (Mammana *et al*., 2010), it was carried out a study on the diameters of Mohr's circles and increments of residual stresses between the mentioned zones, which have no background in literature. The set of observations allowed to identify that when the depth of cut increases, these alloys exhibit different behaviors regarding to the tensors, stress increments and Mohr's circle diameters generated by HSM. Finally, this study

Corresponding Author: F.V. Díaz, Departamento de Ingeniería Electromecánica-Departamento de Ingeniería Industrial, Facultad Regional Rafaela, Universidad Tecnológica Nacional, Acuña 49, 2300 Rafaela, Argentina, Tel.: +54 3492 432710; Fax: +54 3492 422880

proposes a thorough analysis on the causes of such behaviors.

MATERIALS AND METHODS

This study was carried out in the year 2016 at the Departamento Ingeniería Electromecánica, Facultad Regional Rafaela, Universidad Tecnológica Nacional of Argentina.

As mentioned above, this study was carried out from samples of AA 6082-T6 and AA 7075-T6 aluminum alloys, which were cut from rolling plates of 4 mm thick. The micro-hardness of these plates, evaluated from different points, averaged 108 HV0.5 and 186 HV0.5 and the Ultimate Tensile Strength (UTS): 340 MPa and 564 MPa, respectively. From these values, AA 6082-T6 and AA 7075-T6 aluminum alloys can be considered of middle and high mechanical strength.

The dimensions of the tested samples were 110 mm×40 mm×4 mm. Before the HSM tests, the samples were heat treated in order to remove the residual stresses generated during the rolling process. The temperature and time of the thermal treatment were 300°C and 80 min, respectively. In the tests of HSM, a self-balanced face mill of 63 mm in diameter was used. This cutting tool incorporates five inserts (Palbit SEHT 1204 AFFN-AL SM10) of tungsten carbide. The rake, clearance and entrance angles were 45°, 7° and 45°, respectively. The cutting speed was set at V = 1000 m/min and the feed rate at f = 0.04 mm/tooth. Furthermore, the depth of cut was varied from d = 1.00 mm to d = 1.25 mm in order to evaluate the residual stress variation in both cutting zones. It should be noted that the feed per tooth is the linear displacement of the sample when the face mill rotates 1/5 of revolution.

As mentioned above, the tests were performed on a numerically controlled vertical milling machine (Clever CMM-100). An upper view of the relative position of the tested sample with respect to the cutting tool is shown in Fig. 1a. Figure 1b shows the conventional ($x > 0$, y) and climb ($x < 0$, y) cutting zones generated by central cutting and also, the position of the points A (x = -14 mm, y = 0 mm) and B (x = 14 mm, y = 0 mm), which are located in the centroids of the mentioned zones.

All details of the measurement procedure, which corresponds to a micro-indent technique, can be consulted in previous studies (Díaz *et al*., 2010; Díaz and Mammana, 2012). In this technique, a series of micro-indents is introduced into the surface evaluated; then, the micro-indent coordinates are measured, before and after a treatment of thermal relaxation, using a high-precision Universal Measuring Machine (UMM). It is important to note that these machines are very flexible, allowing the realization of different types of measurements on mechanical components, including the determination of the orthogonal coordinates (x, y, z) at any point from the inclusion of a high-accuracy microscope on the main head of the machine (Curtis and Farago, 2007).

Figure 2 shows the state of residual stress at a point corresponding to the surface generated (point P). For obtaining the different components of stress for any point of such surface, eight micro-indents must be introduced. Each micro-indent pair corresponds to a corner of an imaginary square whose centroid is the point to be evaluated (Díaz and Mammana, 2012). In this study, the introduction of such micro-indents was performed using a high accuracy mechanical device, which is mounted on the UMM (Díaz *et al*., 2010). As previously mentioned, the micro-indent coordinates were measured, before and after a distension treatment (300°C and 80 min), using a UMM (GSIP MU-314). Then, through the processing of these coordinates (Mammana *et al*., 2010), it is possible to obtain the components of residual strain ε_x, ε_y and γ_{xy}, which correspond to the centroid of the square mentioned. Afterwards, through these components and assuming

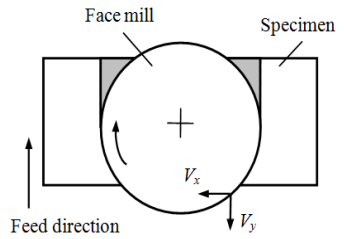

(a)

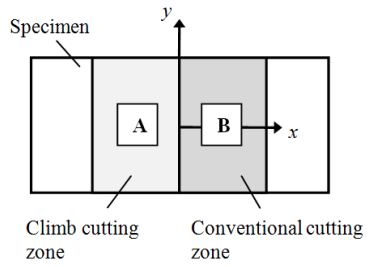

(b)

Fig. 1: (a): Upper view of the tool-sample system and; (b): cutting zones introduced

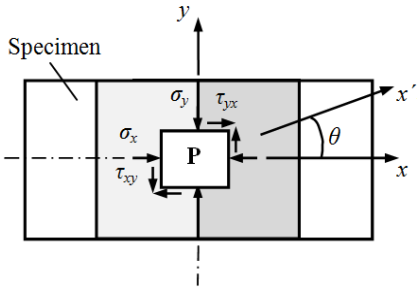

Fig. 2: Residual stress state

that the milled surface is under conditions of plane stress (Gere, 2001), the stress components, in the case of a homogeneous, isotropic and linear elastic material, can be expressed as:

$$\sigma_{x'} = \frac{\sigma_x + \sigma_y}{2} + \frac{\sigma_x - \sigma_y}{2}\cos 2\theta + \tau_{xy} \cdot \sin 2\theta$$
$$\tau_{x'y'} = -\frac{\sigma_x - \sigma_y}{2}\sin 2\theta + \tau_{xy} \cdot \cos 2\theta \quad (1)$$

where, σ_x, σ_y and τ_{xy}, obtained from ε_x, ε_y and γ_{xy}, are the residual stress components corresponding to the original reference system and θ is the angle associated with the direction of evaluation with respect to the reference axis x (Fig. 2).

Finally, the measurement error of this procedure was estimated to be ±0.9 MPa (Díaz *et al*., 2010). Regarding the micro-indent coordinates, these were measured within a temperature range of 20±0.2°C, with less variation than 0.01°C/min. It is noteworthy that if this variation is greater than the value mentioned, the measurement error would increase significantly.

RESULTS AND DISCUSSION

In each material, for each significant point of the generated surfaces, it was possible to evaluate the residual stress states introduced by HSM through different depths of cut. As mentioned above, the representative points are located in the centroids of the conventional and climb cutting zones (Fig. 1b).

Figure 3 and 4 show the normal components of residual stress associated with the reference and principal directions, respectively. It should be noted that the principal directions are the orthogonal directions where the normal components reach their maximum and minimum values (Gere, 2001). As it can be observed in these figures, the stresses are compressive independently of the material, centroid and combination of process parameters evaluated. This is because, in the case of face milling, the secondary cutting edge interacts with the sample intermittently, which generates a higher tensile strain behind the cutting-edge (Trent, 1991). Then, this zone is unloaded, leading to a state of compressive stress.

Furthermore, the higher stresses in absolute value correspond to the centroid of the conventional cutting zone (Point B), independently of the material and of the combination of process parameters, which would be the result of that, in this zone, the feed rate direction and the V_y component of the cutting speed are opposite (Díaz *et al*., 2010).

Regarding the influence of the material, the stresses generated in samples of 6082-T6 were more compressive than those obtained in samples of alloy 7075-T6. This would occur, as described in previous works (Díaz *et al*., 2010; Mammana *et al*., 2010), due

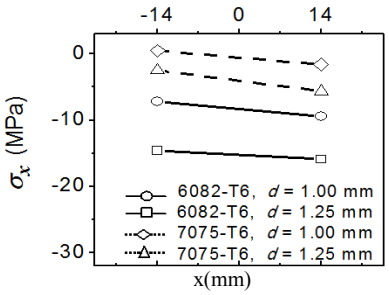

(a)

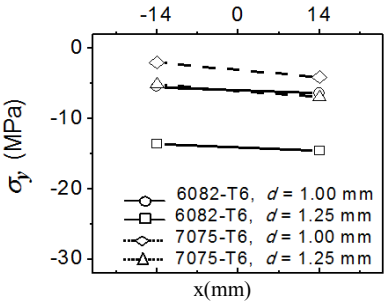

(b)

Fig. 3: Normal components; (a): σ_x and; (b): σ_y in centroids A (x = -14 mm) and B (x = 14 mm) (cutting speed, V = 1000 m/min; feed rate, f = 0.04 mm/tooth)

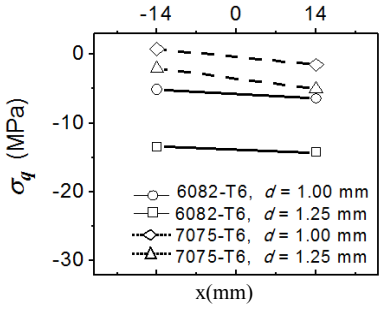

(a)

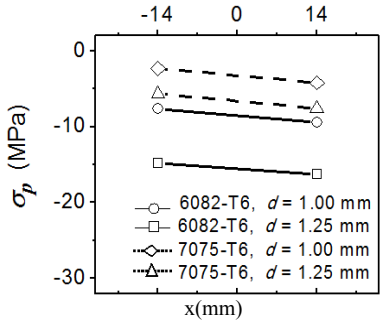

(b)

Fig. 4: Normal components; (a): σ_q and; (b): σ_p in centroids A (x = -14 mm) and B (x = 14 mm) (cutting speed, V = 1000 m/min; feed rate, f = 0.04 mm/tooth)

Table 1: Stress variation between the centroids B and A

	$\Delta\sigma$ (MPa)			
	6082-T6		7075-T6	
Components	d = 1 mm	d = 1.25 mm	d = 1 mm	d = 1.25 mm
σ_x	-2.23	-1.31	-2.10	-3.16
σ_y	-0.89	-0.94	-2.10	-1.80
σ_m	-2.06	-1.12	-2.10	-2.48
σ_p	-1.84	-1.43	-1.88	-1.92
σ_q	-1.28	-0.83	-2.32	-3.04

to different fractions of thermal energy transferred from the primary deformation zone to the surface machined. This fact would respond to that the alloys have different thermal conductivity, being this property higher for the case of the alloy 6082-T6.

In both materials, when the depth of cut increases, more compressive stresses are obtained, which is a product of increments in the cutting forces (mechanical effect). It is noteworthy that the residual stress increments are higher for the case of the alloy 6082-T6. On the other hand, if the more compressive principal stress (σ_p) is isolated to be analyzed (Fig. 4b), it can be observed that, in all combinations, the modes of change are very similar, presenting a clear parallelism between segments. This fact indicates the same behavior for both materials when the principal direction is analyzed. Furthermore, Table 1 shows the values of the stress increments between both centroids, for each combination of material and parameter d. This table includes the normal component σ_m, which represents the average value of the stress tensor taking into account all directions. In addition, this component corresponds to the center of Mohr's circle generated (Gere, 2001). In this table, it can be observed that, for the principal component σ_p, all increments are within a very small range (0.5 MPa).

In addition, in the mentioned table, the values for d = 1 mm are similar for both materials. However, when the depth of cut increases (25%), both materials show opposite behaviors. In the alloy 6082-T6, the stress increments obtained between both centroids decrease, which would occur due to a greater increment in the thermal effect (associated with tensile stress introduction) in the point B with respect to A (Díaz *et al*., 2013). In the alloy 7075-T6, the effect is contrary: the stress variations between centroids are higher when the depth of cut increases, which would be due to a greater increment in the mechanical effect (associated with compressive stress introduction) also at the point B with respect to A.

Including in this analysis the Mohr's circles associated with both centroids, which were studied in a previous work (Mammana *et al*., 2010), it can be noted that each alloy has a particular behavior for each combination of process parameters proposed. Table 2 shows the diameters of the mentioned Mohr's circles for the different combinations of centroid, alloy and depth of cut. In this table is observed that, for each combination of material and centroid, the diameters decrease, except for the alloy 7075-T6 in the point A. It is important to note that if the diameter decreases, the residual stress anisotropy, corresponding to the state evaluated, also decreases. It is noteworthy that the concept of anisotropy only refers to the range of values containing all normal components in the different planar axes (Gere, 2001).

Table 2: Diameters of Mohr's circles (MPa)

Alloy	Depth of cut	Point A	Point B
6082-T6	d = 1.00 mm	2.50	3.06
	d = 1.25 mm	1.43	2.02
7075-T6	d = 1.00 mm	3.13	2.69
	d = 1.25 mm	3.64	2.53

This phenomenon indicates that when the depth of cut increases, the normal components tend to be grouped into smaller intervals and besides, to show a more homogeneous directional behavior. This feature is more pronounced in the alloy 6082-T6, which also presents, as was mentioned previously, a reduction of stress increments between centroids when the depth of cut increases. Therefore, it is possible establish that, when a slight modification toward situations of more severe cutting is proposed, the alloy 6082-T6 seems to respond better than the alloy 7075-T6, regardless of the cutting zone evaluated.

CONCLUSION

The micro-indent method used in this study allowed to analyze different normal components of residual stress in representative points of several milled surfaces. In all cases, these components, introduced by HSM, were compressive and low. Through the analysis carried out at different depths of cut, it was possible to detect that the normal components are slightly higher in the conventional cutting zone, which would be due to the larger plastic deformation generated when the direction of the V_y component of cutting speed is opposite to the feed rate direction. Moreover, the levels reached by the alloy 6082-T6 were consistently greater (in absolute value) than the alloy 7075-T6, which would be due to small differences, in the heat flow from the primary deformation zone towards the new surface, because the former has higher thermal conductivity.

Although in the alloy 7075-T6, the residual stresses are lower, from the stress increments observed between

centroids, it was possible to detect, for the alloy 6082-T6, a more homogenous stress behavior regarding both cutting zones when the depth of cut increases. Complementing this analysis with the study of the stress tensors through the diameters of Mohr's circles, it can be demonstrated how the aforementioned alloy, when the milling is more severe, seems to achieve a best adaptation, presenting a less stress anisotropy in the different zones of the surfaces generated. This would respond to a best combination of mechanical and thermal properties, for the alloy 6082-T6, in relation to the change in the cutting conditions proposed in this study.

ACKNOWLEDGMENT

The authors acknowledge the financial support of Universidad Tecnológica Nacional and Consejo Nacional de Investigaciones Científicas y Técnicas of Argentina.

REFERENCES

Abrão, A.M., J. Silva Ribeiro and J. Paulo Davim, 2011. Surface Integrity. In: Paulo Davim, J. (Ed.), Machining of Hard Materials. Springer-Verlag, London, pp: 115-141.

Brinksmeier, E., J.T. Cammett, W. König, P. Leskovar, J. Peters and H.K. Tönshoff, 1982. Residual stresses-measurement and causes in machining processes. CIRP Ann-Manuf. Techn., 31(2): 491-510.

Curtis, M.A. and F.T. Farago, 2007. Handbook of Dimensional Measurement. Industrial Press Inc., New York.

Cus, F., U. Zuperl and V. Gecevska, 2007. High speed end-milling optimisation using particle swarm intelligence. J. Achiev. Mater. Manuf. Eng., 22(2): 75-78.

Díaz, F.V., R.E. Bolmaro, A.P.M. Guidobono and E.F. Girini, 2010. Determination of residual stresses in high speed milled aluminium alloys using a method of indent pairs. Exp. Mech., 50(2): 205-215.

Díaz, F.V. and C.A. Mammana, 2012. Study of Residual Stresses in Conventional and High-Speed Milling. In: Filipovic, L.A. (Ed.), Milling: Operations, Applications and Industrial Effects. Nova Science Publishers Inc., New York, pp: 127-155.

Díaz, F., C. Mammana and A. Guidobono, 2012. Evaluation of residual stresses induced by high speed milling using an indentation method. Modern Mech. Eng., 2(4): 143-150.

Díaz, F.V., C. Mammana and A.P. Guidobono, 2013. Study of residual stresses from two machining protocols using an indentation method. Int. J. Mech. Eng. Appl., 1(4): 87-92.

Gere, J.M., 2001. Mechanics of Materials. 5th Edn., Brooks/Cole, Pacific Grove, CA.

Mammana, C.A., F.V. Díaz, A.P.M. Guidobono and R.E. Bolmaro, 2010. Study of residual stress tensors in high-speed milled specimens of aluminium alloys using a method of indent pairs. Res. J. Appl. Sci. Eng. Technol., 2(8): 749-756.

M'Saoubi, R., J.C. Outeiro, H. Chandrasekaran, O.W. Dillon Jr. and I.S. Jawahir, 2008. A review of surface integrity in machining and its impact on functional performance and life of machined products. Int. J. Sust. Manuf., 1(1/2): 203-236.

Pare, V., G. Agnihotri and C. Krishna, 2015. Selection of optimum process parameters in high speed CNC end-milling of composite materials using meta heuristic techniques – a comparative study. J. Mech. Eng., 61(3): 176-186.

Rao, B. and Y.C. Shin, 2001. Analysis on high-speed face-milling of 7075-T6 aluminum using carbide and diamond cutters. Int. J. Mach. Tool. Manu., 41(12): 1763-1781.

Schulz, H., 1996. High Speed Machining. Carl Hanser, Munich.

Trent, E.M., 1991. Metal Cutting. 3rd Edn., Butterworth/ Heinemann, London.

Yao, C.F., Z.C. Yang, X.C. Huang, J.X. Ren and D.H. Zhang, 2012. The study of residual stresses in high-speed milling of titanium alloy TC11. Adv. Mater. Res., 443-444: 160-165.